IJOCIT

Review Paper

Brain Tumor Detection Using Ripplet and Support Vector Machine (SVM)

Hamed Moradjou [1,*]
Masoud Bekravi [2]

Abstract

The main objective of the method is to automatically segment and detect brain tumor using Ripplet and Support Vector Machine. An automatic segmentation of brain images is needed to correctly segment tumor from other brain tissues. Accurate detection of size and location of brain tumor plays a vital role in the diagnosis of tumor. This method propose an classification and the efficiency in representing edges and textures brain image for tumor detection which utilizes the complementary and redundant information from the Computed Tomography (CT) image and Magnetic Resonance Imaging (MRI) images. The reason for going onto image classification is that, in the medical image processing, different sources of images produce complementary information and so one has to fuse all the sources of images to get more details required for the diagnosis of the patients. Hence this ripplet uses the information provided by the CT image and MRI images there by providing a resultant fused image which increases the efficiency of tumor detection. Segmentation of the fused image is performed using thresholding. Feed Forward support vector machine is used to automatically detect brain tumor from segmented brain image.

Keywords: Computed Tomography, Support Vector Machine (SVM), Ripplet, Magnetic Resonance Imaging (MRI).

1   Department of Computer Engineering, Germi Branch, Islamic Azad University, Germi, Iran
2   Department of Computer Engineering, Ardabil Branch, Islamic Azad University, Ardabil, Iran
*   Corresponding Author: moradjou@gmail.com

1. Introduction

Magnetic Resonance Imaging (MRI) is a non-invasive imaging technique which provides high contrast images of different anatomical structures. It provides better discrimination of soft tissues than other medical imaging techniques. MRI is frequently being used in detection and the diagnosis of brain tumors [1, 14]. Brain image classification in MRI is an active research area [2, 3, and 7]. The classification of different brain images help in correct treatment. Existing techniques can be broadly classified into supervised [5,7] and unsupervised [9, 10] techniques. Un-supervised techniques do not work in complex scenarios and are based on certain assumptions, such as cluster size etc. The supervised classification technique work on the principle of training and testing data. These techniques provide better classification accuracy than others [5]. In medical images, noise intensities and textural properties may vary from image to image which may result in poor classification accuracy for supervised methods. These limitations however can be addressed by using invariant features and better classifiers. Various techniques for classification of images are in literature [2, 11]. Gray level thresholding and morphological features based technique does not provide satisfactory results due to complex brain structure and sudden variations in intensities. Segmentation based schemes [11], fail to work if the abnormalities in the brain are not possible to be segmented spatially. Furthermore, the statistical and geometrical variations in brain images limit the performance of these schemes. A brain tumor is a mass of abnormally growing cells in the brain or skull. It can be benign (noncancerous) or malignant (cancerous). Unlike other cancers, a cancer arising from brain tissue (a primary brain cancer) rarely spreads. All brain tumors whether benign or malignant are serious [1]. A growing tumor eventually will compress and damage other structures in the brain. There are two types of brain tumors: primary and secondary. Primary tumors begin in brain tissue, while secondary tumors spread to the brain from another part of the body accurate detection of size and location of brain tumor plays a vital role in the diagnosis of tumor. In the last two decades medical science has seen a revolutionary development in the field of biomedical diagnostic imaging. The current technologies in the field of artificial intelligence and computer vision technologies have been very effectively put into practice in applications such as diagnosis of diseases like cancer through medical imaging. The main emphasis of the latest developments in medical imaging is to develop more reliable and capable algorithms which can be used in real time diagnosis of tumors. [2]

The detection of brain tissue and tumor in MR images and CT scan images has been an active research area. Segmenting and detection of specific regions of brain containing the tumor cells is considered to be the fundamental problem in image analysis related to tumor detection[3]. This method seeks to bring out the advantages of segmentation of CT scan images and MR images through image fusion. Image fusion is one of the most commonly used methods in medical diagnosis. It merges the multimodal images to provide additional information. Medical imaging image fusion, usually involves combining information of multi modalities such as magnetic resonance image (MRI), computed tomography (CT), positron emission tomography (PET), and single photon emission computed tomography (SPECT).[4] Image fusion is more general solution to a number of applications in image processing where high spatial and spectral information are required in a single image. Image fusion is used to overcome the observational constraints, which account for the disability to build such instruments to provide such information. [5]

2. Ripplet Transform

To generalize the scaling law of the Curvelet transform a new transform called Ripplet transform was introduced. The Ripplet transform has the following capabilities: Multi-resolution, Good localization, High Directionality, general scaling and support, anisotropy, fast coefficient decay. Ripplet transform can represent images more efficiently than DCT and Discrete wavelet transform (DWT) when the compression ratio is high.

Curvelet transform uses a parabolic scaling law to achieve anisotropic directionality. The anisotropic property of Curvelet transforms guarantees resolving 2D singularities along C2 curves. But, it is not clear why parabolic scaling was chosen for Curvelet to achieve anisotropic directionality. We proposed a new transform called Ripplet transform Type I (Ripplet-I), which generalizes the scaling law. Ripplet-I transform generalizes Curvelet transform by adding two parameters, i.e., support c and degree d. These new parameters, i.e., support c and degree d, provide Ripplet-I with anisotropic capability of representing 2D singularities along arbitrarily shaped curves [11]. We can define the scaling law in a broader scope and more flexible way. The Ripplet function can be generated as the same way as the 2D Curvelet:

$$\hat{\rho}_{\vec{ab\theta}}(\vec{\chi}) = \rho_{a\vec{00}}(R_\theta(\vec{\chi} - \vec{b})$$

Where $\rho_{a00^-}(\vec{\chi})$ the ripplet element is function and $R_\theta = \begin{bmatrix} cos\theta & sin\theta \\ -sin\theta & cos\theta \end{bmatrix}$ is the rotation matrix. We define the element function of ripplet in frequency domain as

$$\hat{\rho}_a(r,\omega) = \frac{1}{\sqrt{c}} a^{\frac{1+d}{2d}} W(a.r) V\left(\frac{a^{\frac{1}{d}}}{c.a}\omega\right)$$

Where $\rho_a^\wedge(r,\omega)$ are the Fourier transform of $\rho_{a00^-}(\vec{\chi})$, W(r) is the „radial window" on [1/2,2] and V(x) is the „angular window" on [-1, 1]. These two windows partition the polar frequency domain into „wedges" as shown in Fig. 1.

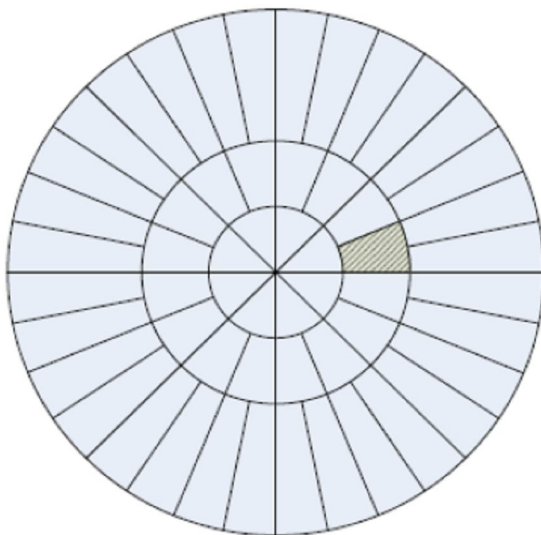Figure 1. The tiling of polar frequency domain. The shadowed 'wedge'

The set of functions $\{\rho_{ab-\theta}^\wedge\}$ is defined as Ripplet functions or ripplets for short, because in spatial domain these functions have ripple- like shapes. c determines the support of ripplets and d is defined as the degree of ripplets. Fig. 2 shows ripplets with different c and different d in spatial domain. From Fig. 2, we can see that ripplet functions decay very fast outside the effective region, which is an ellipse with the major axis pointing in the direction of the ripplet. The major axis is defined as the effective length and the minor axis, which is orthogonal to the major axis, is the effective width. The values of c and d will actually affect the effective length and width of ripplets in

spatial domain. The effective region has the following properties for its length and width: $Width \approx c \times length^d$. For fixed d, the larger c is, the shorter the width is and the longer the length is. When c is fixed and d gets larger, the width gets shorter and the length is elongated. The customizable effective region tuned by support c and degree d bespeaks the most distinctive property of ripplets – the general scaling. For c = 1, d = 1, both axis directions are scaled in the same way. So ripplet with d = 1 will not have the anisotropic behavior. For d > 1, the anisotropic property is reserved for ripplet transform. For d = 2, ripplets have parabolic scaling; for d = 3, ripplets have cubic scaling; and so forth. Therefore, the anisotropy provides ripplets the capability of capturing singularities along arbitrary curves. The ripplets as the generalization of curvelet have almost all the properties of curvelet except the parabolic scaling. Ripplets can get multi-resolution analysis of data. For each scale, ripplets have different compact supports such that ripplets can localize the singularities more accurately. Ripplets are also highly directional to capture the orientations of singularities.
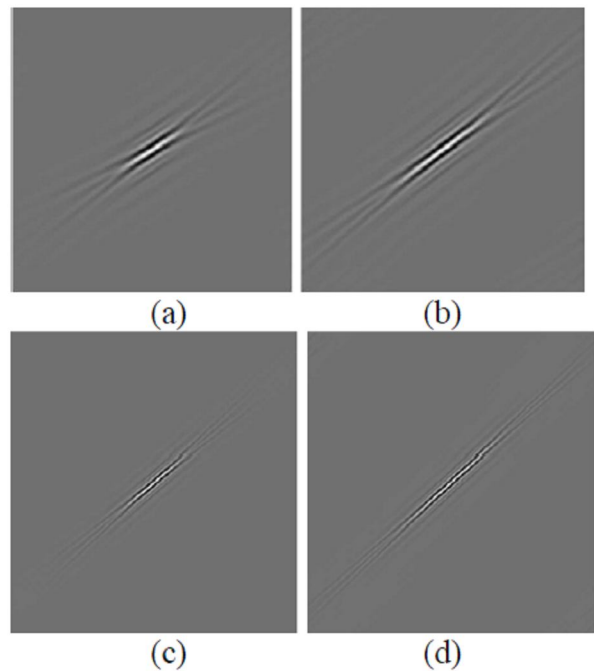

Figure 2. Ripplet in spatial domain with different degrees and support which are all located in the center, i.e., b=0.(a) a=3, θ=3 π /16,, c=1, d=2, called curvelet particularly. (b)a=3, θ = 3 π /16, c=1.5, d=2. (c) a=4, θ = 3 π /16, c=1, d=4. (d) a=4, θ = 3 π /, c = 1.5, d = 4.

3. Discrete Ripplet Transform

We introduced ripplets and continuous ripplet transform. Digital image processing needs discrete transforms instead of continuous transforms. Discretization of ripplet transform is proposed and analyzed in this section. The discretization of continuous ripplet transform is actually based on the discretization of the parameters of ripplets, which is similar to discrete curvelet transform [16]. For the scale parameter a, we sample at dyadic intervals. The position parameter b and rotation parameter b and rotation parameter θ are sampled at equal spaced intervals. $a, \vec{b}$ and θ are substituted with discrete parameters $a_j, \vec{b_k}$ and θ_l, which satisfy that $a_j = 2^{-j}, \vec{b_k} = [c \cdot 2^{-j} \cdot k_1, \ 2^{-j/d} \cdot k_2]^T$ and $\theta_l = \frac{2\pi}{c} \cdot 2^{-\lfloor j(1-1/d) \rfloor} \cdot l$ where $\vec{k} = [k_1, \ k_2]^T$ denotes the transpose of a vector and $j, k_1, k_2, l \in \mathbb{Z}$ The degree of ripplets can take value from R. Since any real number can be approximated by rational numbers, we can represent d with $d = n/m, \quad m \neq \cdot \in \mathbb{Z}$. Usually, we prefer $n, m \in N$ and n;m are both primes. In the frequency domain, the corresponding frequency response of ripplet function is in the form:

$$\hat{\rho}_j(r, \omega) = \frac{1}{\sqrt{c}} \, a^{\frac{m+n}{2n}} W(2^{-j} \cdot r) V(\frac{1}{c} \cdot 2^{-\lfloor j \frac{m-n}{n} \rfloor} \cdot \omega - l)$$

Where W and V satisfy admissibility conditions as below.

$$\sum_{j=0}^{+\infty} |W(2^{-j} \cdot r)|^2 = 1$$

$$\sum_{l=-\infty}^{+\infty} |V(\frac{1}{c} \cdot 2^{-\lfloor j(1-1/d) \rfloor} \cdot \omega - l)|^2 = 1, \quad \text{given } c, \, d \text{ and } j$$

The `wedge' corresponding to the ripplet function in the frequency domain is

$$H_{j,l}(r, \theta) = \{2^j \leqslant |r| \leqslant 2^{2j}, |\theta - \frac{\pi}{c} \cdot 2^{-\lfloor j(1-1/d) \rfloor} \cdot l| \leqslant \frac{\pi}{2} 2^{-j}\}.$$

In discrete case, we can have better understanding about the parameters c and d. The parameter c controls the number of directions in the high-pass bands. d controls how the number of directions changes across bands. For fixed c, d helps to control the resolution in directions at each high-pass band. Given d, c controls the number of directions at all high-pass bands. c and d determine the final number of directions at each band together. The discrete ripplet transform of an M * N image $f(n_1, n_2)$ will be in the form of

$$R_{j,\vec{k},l} = \sum_{n_1=0}^{M-1} \sum_{n_2=0}^{N-1} f(n_1, n_2) \overline{\rho_{j,\vec{k},l}(n_1, n_2)},$$

Where $R_{j,k,l}$ are the ripplet coefficients? The image can be reconstructed through inverse discrete ripplet transform:

$$\tilde{f}(n_1, n_2) = \sum_j \sum_{\vec{k}} \sum_l R_{j,\vec{k},l} \rho_{j,\vec{k},l}(n_1, n_2).$$

4. Image Segmentation

The enhanced image undergoes the process of segmentation done using morphological operators. The segmentation is the process of partitioning the image into multiple segments. It is to simplify the representation of the image. The enhanced image is been segmented using morphological gradient operators.

4.1. Morphological Operators

The fundamental operators in morphology are dilation, erosion, opening and closing. Choosing the SE is important in morphological image processing because the size, shape and the direction of the SE determines the final result. To detect the complex edges we need advanced SEs. The basis is gathering several SEs in one square window.

4.2. Image Reconstruction

The morphological operator is been used to reconstruct the vessel segments. A correct selection of the marker and mask images allows the generation of binary images. Reconstructing the mask image (I) from marker image (J) is the union of connected components of the mask image which contain at least a pixel of marker image.

$$\rho_I(J) = \bigcup_{J \cap I_k \neq \emptyset} I_k$$

5. Classification MRI BRAIN IMAGE using SVM

SVM is a margin based classifier which achieve superior classification performance compared to other algorithms. The basic principle of SVM is to search for optimal hyper plane with maximal distance of the nearest samples from each class. Let the total images to be classified are K, where k = 1,2,…,K and their respective weighted features are $[f_1, f_2, \dots, f_k]$ The aim is to classify these images into four classes (normal, glioma, sarcoma and meningioma). As discussed earlier, conventional SVM is designed for binary classification. However, multiclass SVM is also in practice. Various techniques have been proposed for modifying binary SVMs to multi-class SVMs. A detailed review of all these algorithms is given in [12]. One-versus-all is the simplest and one of the earliest extensions of SVM for multiclass problems [20]. One-vs all technique is proven a robust and accurate method for well-tuned binary classifiers [20]. In this method, for a K class problem K binary SVM classifiers are required. For ith binary SVM classifier, class i is considered as the positive class whereas the remaining K-1 classes are considered as negative. Another approach is called the one-versus-one multiclass SVM [12]. Although this approach can effectively decrease the un- classifiable regions that occur in the one-against all SVMs, the unclassifiable regions still exists. Unlike the one-versus-all multiclass SVM, this method constructs k (k-1)/2 binary support vector machines. This scheme determines the class of data by using a voting scheme. The decision function, training procedure and voting mechanism is explained in [19].

6. Result and Discussion

For the proposed method is MR image used as the input image. For the method we are considering only registered images. The input image is given to the preprocessing stage and thereafter to the decomposition stage. Thus obtaining fused resultant image. The Ripplet algorithm is repeated for different wavelets and for different level of decomposition .After obtaining the resultant fused image the classification for the images. MR image slices belonging to sarcoma and meningioma classes, respectively. It is important to note that the images of the same class are sometimes quite different (in

terms of texture, geometrical and statistical properties) which results in overlapping features. The problem of overlapping features is countered by applying Ripplet transform.

Figure 3. Input image

Final Fused image is used to extract tumor region after segmentation using support vector machine algorithm. Skull stripping is performed on the segmented image.
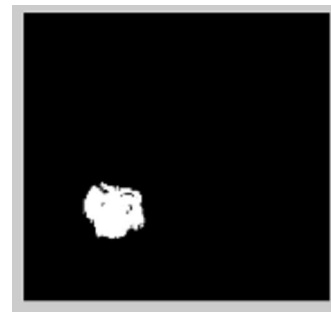

Figure 4. Skull Stripped Image

Figure 5. Tumor

Boundary and area of the tumor region is calculated and plotted in the fused image by Ripplet transform.
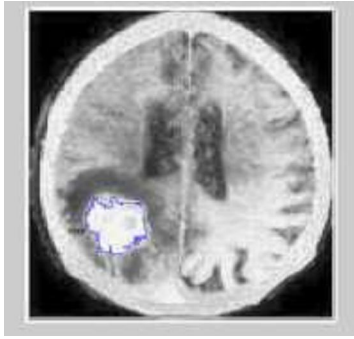
Figure 6. Area Detected in Image

The performance of our proposed technique is compared with the existing schemes by performing quantitative analysis. A classification system on any occasion can either generate false result to identify an abnormality or it may also classify an abnormality which is not present. The probability that classification test is correctly performed is known as accuracy. The proposed and existing technique's accuracy is given for the multi-class problem. The classification results are also tested against different scaling and orientation values.

$$Accuracy = \left(\frac{T_p + T_n}{T_p + T_n + F_p + F_n} \right) \times 100$$

7. Conclusion

A technique is proposed for the MRI brain image classification using Ripplet transform for tumor detection, invariant moments and the multiclass SVM. The proposed technique classifies between normal and different classes of abnormal images. Ripplet transform is used to assign weights to different feature values based on its discrimination capability. The multi class SVM provides better classification accuracy even if the features of different classes have overlapping boundaries. Simulation results show the significance of the proposed technique over state of art existing techniques.

References

[1] Hakyemez, B., C. Erdogan, N. Bolca, N. Yildirim, G. Gokalp, and M. Parlak, (2006). Evaluation of di®erent cerebral mass lesions by perfusion-weighted MR imaging," *Journal of Magnetic Resonance Imaging*, Vol. 24, No. 4: 817-824.

[2] Lau, P. Y., F. C. T. Voon, and S. Ozawa, (2006). The detection and visualization of brain tumors on T2-weighted MRI images using multiparameter feature blocks," International Conference of the Engineering in Medicine and Biology Society, 5104-5107.

[3] Zhang, Y., S. Wang, and L. Wu, (2010). A novel method for magnetic resonance brain image classification based on adaptive chaotic PSO," Progress In Electromagnetics Research, Vol. 109, 325-343.

[4] Zhang, Y., L. Wu, and S. Wang, (2011). Magnetic resonance brain image classification by an improved artificial bee colony algorithm," Progress In Electromagnetics Research, Vol. 116, 65-79.

[5] Zhang, Y. and L.Wu, (2012). An MR brain images classi¯er via principal component analysis and kernel support vector machine," Progress In Electromagnetics Research, Vol. 130, 369-388.

[6] El-Dahshan, E.-S., T. Hosny, and A. M. Salem, (2010). Hybrid intelligent techniques for MRI brain images classification," *Digital Signal Processing*, Vol. 20, No. 2, 433-441.

[7] Das, S., M. Chowdhury, and M. K. Kundu, (2013). Brain MR image classification using multi-scale geometric analysis of ripplet," *Progress In Electromagnetics Research*, 137: 1-17.

[8] Malthouse, E. C., (1998). Limitations of nonlinear PCA as performed with generic neural networks," *IEEE Transactions on Neural Networks*, Vol. 9, No. 1, 165-173.

[9] Chaplot, S., L. M. Patnaik, and N. R. Jagannathan, (2006) Classification of magnetic resonance brain images using wavelets as input to support vector machine and neural network," *Biomedical Signal Processing and Control*, Vol. 1, No. 1, 86-92.

[10] Yeh, J.-Y. And J. C. Fu, (2008). A hierarchical genetic algorithm for segmentation of multi-spectral human-brain MRI", *Expert Systems with Applications*, Vol. 34, No. 2, 1285-1295.

[11] Shelvy, P. T., V. Palanisamy, and T. Purusothaman, (2011). Performance analysis of clustering algorithms in brain tumor detection of MR images," *European Journal of Scientific Research*, Vol. 62, No. 3, 321-330.

[12] Othman, M. F. and M. A. M. Basri, (2011). Probabilistic neural network for brain tumor classification," International Conference on Intelligent Systems, Modelling and Simulation, 136-138.

[13] Joshi, D. M., N. K. Rana, and V. M. Misra, (2010). Classification of brain cancer using artificial neural network," International Conference on Electronic Computer Technology, 112-116.

[14] Zacharaki, E. I., S. Wang, S. Chawla, D. S. Yoo, R. Wolf, E. R. Melhem, and C. Davatzikos, (2009). MRI-based classification of brain tumor type and grade using SVM-RFE," IEEE International Symposium on Biomedical Imaging: From Nano to Macro, 1035-1038.

[15] Cortes, C. and V. Vapnik, (1995). "Support vector networks," *Machine Learning*, Vol. 20, No. 3, 273-297.

[16] Hu, M. K., (1962). "Visual pattern recognition by moment invariants" *IRE Transactions on Information Theory*, Vol. 8, No. 2, 179-187.

[17] [Amadasun, M. and R. King, (1989). Textural features corresponding to textural properties," *IEEE Transactions on Systems, Man and Cybernetics*, Vol. 19, No. 5, 1264-1274.

[18] Vapnik, V., (1995). the Nature of Statistical Learning Theory, *Springer, New York*, USA.

[19] Javed, U., M. M. Riaz, T. A. Cheema, and H. M. F. Zafar, (2013). Detection of lung tumor in CE CT images by using weighted support vector machines," International Bhurban Conference on Applied Sciences and Technology, 113-116.

[20] Horng, M. H., (2009). Multi-class support vector machine for classification of the ultrasonic images of supraspinatus," *Expert Systems with Applications*, Vol. 36, No. 4, 8124-8133.